Geophys. J. Int. (1999) **138,** 717–726

Shape-induced pseudo-single-domain remanence

Karl Fabian[1] and Alex Hubert[2,*]

[1] *FB Geowissenschaften, Universität Bremen, Postfach* 330 440, 28334 *Bremen, Germany. E-mail: karl.fabian@uni-bremen.de*
[2] *Institut für Werkstoffwissenschaften der Universität Erlangen-Nürnberg, Erlangen, Germany*

Accepted 1999 April 12. Received 1999 April 12; in original form 1998 November 11

SUMMARY

Models of uniaxial hard magnetic particles show that irregularly shaped grains possess a considerable equilibrium remanence due to domain imbalance. This remanence decreases approximately as L^{-1} with grain size L and is very stable with respect to alternating field and thermal demagnetization. It is therefore likely to be a major source of pseudo-single-domain remanence in rocks. Using the methods of domain theory, the range of possible remanences in irregularly shaped uniaxial particles with less than five domains is investigated. Even for slightly asymmetric particle geometries the remanence decreases monotonically with grain size. Most two-domain remanences lie above 0.3 M_s. The behaviour of the domain imbalance moments seems to be largely independent of details of the shape asymmetry. Since domain imbalance is a global equilibrium remanence, local remanences due to wall pinning effects can be superimposed without destroying it. This can explain the fact that the remanence of pseudo-single-domain particles appears to be a mixture of independent single- and multidomain-like components.

Key words: magnetic domain, remanent magnetization, rock magnetism.

1 INTRODUCTION AND OVERVIEW

A fundamental task of rock magnetism is to understand the grain-size-dependent magnitude and stability of magnetic remanence in natural materials. Theoretical as well as experimental investigations lead to the discrimination of four grain-size regions which are more or less clearly separated by their magnetic properties (Fig. 1). (i) Magnetic particles (here and in the following 'magnetic particles' means ferro- or ferrimagnetic particles) show *superparamagnetic* behaviour if the energy barrier between different magnetic states is easily overcome by thermal activation energy. (ii) Homogeneously magnetized particles which carry a thermally stable magnetization are called stable single domain (SD) particles. Even though the transition size between superparamagnetic and stable SD particles depends on temperature as well as on the timescale of observation it is relatively clearly defined. SD particles are theoretically well understood. (iii) At very large grain sizes, magnetic particles contain many magnetically homogeneous domains which are separated by domain walls. Such multidomain (MD) particles carry little or no remanence since magnetizations of oppositely magnetized domains more or less completely cancel each other. If some remanence in MD particles remains, it results from restrictions on the movement of domain walls such as domain wall pinning at dislocations or inclusions.

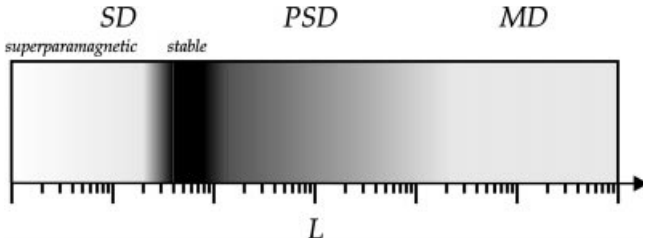

Figure 1. Qualitative particle size classification with respect to remanence as is customary in rock magnetism. SD particles are superparamagnetic at very small grain sizes and cannot carry remanence due to thermal activation. Stable SD particles carry a high remanence, whilst MD particles have a soft and relatively small remanence. In the intermediate region the remanence decreases and shows characteristics of both MD and SD particles. Since here the SD-like remanence fraction is not assumed to be generated by SD particles, it is called PSD remanence. For magnetite the logarithmic length scale ranges approximately from 1 nm on the left to 1 mm on the right. Dark regions indicate high remanence and light regions low remanence.

It was a surprise to rock magnetists when experimental evidence showed that there is no sudden change between SD and MD behaviour, but rather a smooth transition which extends

* Passed away in March 1999.

over a very large grain-size range. The magnetic remanence in this transition region has SD-like as well as MD-like aspects and was called 'pseudo-single-domain' (PSD) remanence by Stacey (1962). PSD remanence is of special interest in rock magnetism since probably by far the largest part of stable remanence in rocks (which contains palaeomagnetic information) is carried by PSD particles. However, despite its importance, there is still no generally accepted theory concerning the nature of PSD remanence. In its appearance as a mixture of SD-like and MD-like remanence components, the SD-like part has not yet been identified beyond doubt. In the following we summarize the main points of PSD phenomenology which we are going to discuss later. A more detailed compilation can be found in Section 12.2 of Dunlop & Özdemir (1997).

A very important property of PSD remanence is its *universality*. PSD behaviour occurs in all kinds of magnetic materials in a large transition size range between SD and MD particles. A general theory of PSD remanence therefore should not be based on special circumstances, which are not ubiquitous in magnetic materials. In other words, PSD remanence should have a simple and natural explanation.

The main rock magnetic effect of PSD remanence is the high intensity of weak-field thermoremanent magnetization (TRM) in particles above the theoretically predicted SD threshold size d_0. According to MD theory, a sudden drop in TRM intensity should occur above d_0, which is not observed (Stacey 1962; Dunlop 1990). Moreover, the variation of TRM with applied field is intermediate between theoretical predictions for SD and MD particles. Also, the coercivity spectrum of weak-field TRM is similar to that of a mixture of SD and MD components.

Saturation-induced remanent magnetization (SIRM), M_{rs}/M_s, as a function of grain size, L, approximately follows a power law. For magnetite the $M_{rs}(L)/M_s$ data for grown crystals as well as for crushed crystals show approximately a $L^{-0.6}$ dependence. However, the linear fit of the data set for crushed particles in the bilogarithmic M_{rs}–L plot is shifted towards larger grain sizes with respect to the fit for grown crystals (Dunlop 1995). This is assumed to be an effect of internal stress, which is more prominent in crushed particles. Similar grain size and stress effects as for M_{rs} have been obtained for the coercive force H_c.

An interesting experimental result indicates that PSD remanence in magnetite is composed of an SD-like and an independent MD-like component. It concerns the behaviour of the PSD remanence of magnetite with respect to low-temperature demagnetization (LTD). The low-temperature (LT) memory, which is the fraction of remanence that survives a cooling–heating cycle through the isotropic point ($\approx$135 K for magnetite; see Hunt *et al.* 1995), shows mainly SD-like behaviour with respect to AF demagnetization, whilst the remanence which was lost during LT demagnetization behaves like that of MD particles during AF demagnetization (Dunlop & Argyle 1991; Heider *et al.* 1992; McClelland & Shcherbakov 1995; Dunlop & Özdemir 1997). Whilst the unblocking of TRM also has separate SD- and MD-like aspects in PSD particle ensembles, the experiments performed by Shcherbakova *et al.* (1996) showed that pTRMs of LT demagnetized PSD ensembles do not behave like SD particles.

Various theories have been proposed to explain the above properties of remanent magnetization in PSD grains. All of these theories are thoroughly reviewed and discussed in Section 12 of Dunlop & Özdemir (1997). Here we therefore only briefly summarize the main ideas that have been put forward to explain parts or all of the PSD phenomenon:

Stacey (1963) proposed the theory of *Barkhausen discreteness* in the position of the domain walls. He assumed that the domain walls in small particles are magnetoelastically bound to defects and only jump between such bound states. Since in zero field the walls therefore cannot arbitrarily vary in order to annihilate the magnetic moment, there remains an uncompensated PSD moment. This theory is supported by the consideration that *magnetic screening* in PSD and multidomain (MD) grains may account for the observed high stability of PSD remanence with respect to AF demagnetization (Xu & Dunlop 1993). The weak point of this explanation is that it fails to explain the SD-like part of PSD remanence as well as the grain-size dependence of M_{rs}. In particular, the high coercivity of small PSD particles, where magnetic screening is less effective, cannot be accounted for.

The theories of *wall moments* or 'PSARKs' claim that the major contribution to PSD remanence results from the magnetization structure within domain walls (Dunlop 1977). In particular, in small particles the domain wall occupies a large portion of the grain (Dunlop 1973). Resulting moments in two-domain grains have been calculated by Stacey & Banerjee (1974). More rigorous 3-D micromagnetic calculations for magnetite show that these moments result only from a magnetization swirl which penetrates the particle and that they decay very rapidly with increasing grain size (Williams & Dunlop 1989, 1990; Fabian *et al.* 1996). The 'PSARK' theory thus has difficulties in explaining the grain-size dependence of M_{rs}. Moreover, in larger particles the interaction between wall moments leads to an even faster decrease of the predictable average M_{rs} as compared to experimental data.

Shcherbakov (1978) realized that the spontaneous remanence carried by cubic uniaxial particles with an odd number of domains—the existence of which was previously found by Craik & McIntyre (1969)—could account for PSD effects. He noted that while cubic particles with an even number of domains do not carry bulk remanence, they may possess a net moment due to their odd number of wall moments. Dunlop (1983) investigated this *domain imbalance* theory in more detail and combined it with the wall moment theory. The problem of this combination is that the domain wall moments decrease too fast, while, according to Shcherbakov and Dunlop, the domain imbalance moments vanish completely for small (two- or four-domain) particles, which in reality have large PSD remanence.

Banerjee (1977) proposes *surface anisotropy* as the predominant source of the high-PSD coercivity. The idea that PSD moments are related to surface moments arises from the observation that the characteristic properties (such as M_{rs} or H_c) of PSD particles show approximately a L^{-1} decrease with grain size L. This trend corresponds to the surface-to-volume ratio, and therefore surface effects seem to be the most natural explanation. However, the postulated surface moments necessarily strongly interact with the volume magnetization, which destroys the favourable L^{-1} grain-size dependence of M_{rs} in a similar manner as in the case of wall moments.

The *nucleation theory* of Halgedahl & Fuller (1980, 1983) starts from domain observations, which show very different states of remanence after AF demagnetization and high-field

hysteresis. They concluded that a major contribution to PSD remanence is SD remanence from particles with a grain size above the theoretical SD limit d_0, which fail to nucleate domain walls (or vortex centres). Assuming a Poisson distribution of such metastable SD particles with grain size, they succeeded in reproducing the grain-size dependence of M_{rs}. This theory has been supported by the calculations of Moon & Merrill (1984), Enkin & Dunlop (1987), Fabian *et al.* (1996) and others, which show that micromagnetic particle models may still have SD states as local energy minima above d_0. However, in pure magnetite particles the SD local energy minimum state becomes unstable at some grain size above which SD particles are then impossible (Fabian *et al.* 1996). Larger metastable SD particles therefore must be stabilized by an additional mechanism (e.g. external or internal stress). Numerical results for titanomagnetite indicate that in this case magnetostriction might be an effective mechanism to inhibit nucleation (Fabian & Heider 1996). In any case, nucleation theory implies that the particle ensemble is actually a mixture of SD and MD particles and remanence is carried mainly by the SD fraction.

Sugiura (1988) proposed explaining PSD remanence as originating from homogeneously distributed, but partly screened, SD-like regions within magnetite grains which were first postulated by Verhoogen (1959). Even though this theory could account for some of the puzzling properties of PSD moments, there is no observational evidence to support the ubiquitous existence of inner regions behaving like SD particles in magnetic materials. Therefore, this theory cannot explain the universality of PSD effects. Moreover, the results of Shcherbakova *et al.* (1996) seem to exclude true SD moments as carriers of PSD remanence.

Here an alternative theory is presented to explain the properties of remanence in PSD particles. This theory questions an assumption that is implicitly made in all of the above theories, namely the assumption that the natural undisturbed state of a particle with one domain wall carries no bulk remanence. It will be shown that this is generally not true. On the contrary, *almost all* particles with one or more domain walls carry bulk remanence of the domain imbalance type—even in their absolute energy minimum.

In order to simplify the calculation of the demagnetizing energy, theoretical investigations of two-domain or multidomain particles have always used grain geometries with parallel magnetically charged surfaces (symmetric geometry). A typical symmetric geometry is shown in Fig. 2(a). However, compared to observed geometrical arrangements in real particles (Fig. 3), such symmetrical shapes are certainly highly idealistic. A characteristic feature of all symmetric particle geometries is that, independent of the specific wall energy γ_0, the remanence of the two-domain state is zero. In more irregularly shaped grains like that in Fig. 2(b), the wall area is a function of wall position. It is therefore obvious that with increasing γ_0 the wall will shift towards a position with less area A, thereby decreasing the total wall energy $\gamma_0 A$ while increasing the demagnetizing energy by generating additional remanence. It is less obvious that even in the case where the wall energy is negligible, the equilibrium two-domain configuration of an irregularly shaped grain will carry remanence.

Assume a particle shape as shown in Fig. 2(b) for a qualitative explanation of this effect. We distinguish two contributions to the magnetostatic energy of the particle: (i) the interaction energy between the top and bottom surfaces, which is approximately the magnetic dipole energy, and (ii) the self-energies of the top and bottom surfaces, which are related to the charge distribution on the respective surfaces.

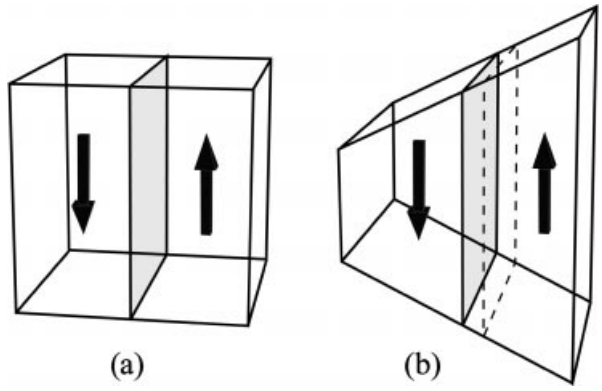

Figure 2. Comparison between equilibrium two-domain states in a cubic particle (a) and an asymmetric trapezoidal particle (b). While the cubic particle has zero remanence, the trapezoidal particle carries an equilibrium remanence of $\approx 0.2 M_s$ in the direction of the right domain if only demagnetizing energies are considered. The dashed line in (b) marks the zero-remanence position of the wall. Taking into account a finite wall energy does not affect the equilibrium position in (a), whilst the wall of particle (b) is shifted further to the left.

Due to the irregular shape, the position $x = x_0$ of the wall at which the two domains have equal volume (that is, the particle's dipole moment or remanence is zero) is shifted to the right of the central position $x = 1/2$. However, for $x = x_0$ there results an imbalance of magnetic charges on each charged surface which leads to an increase of the magnetostatic self-energies of the respective surfaces. The minimum of the self-energies is achieved at $x = 1/2$, where it is true that the net surface charge on each surface is zero, but a considerable magnetic dipole moment is present. The equilibrium wall position, x_{eq}, therefore lies somewhere between the midpoint and x_0, leading to an equilibrium net moment.

The purpose of this article is to give a more detailed and quantitative treatment of this effect and to investigate its implications with respect to PSD remanence.

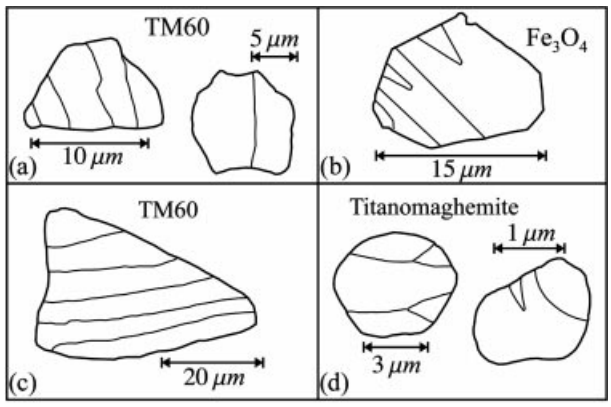

Figure 3. Some schematic cross-sections of natural PSD particles used for Bitter observations. (a) Halgedahl & Fuller (1983); (b) Heider *et al.* (1988); (c) Halgedahl (1991); (d) Geiß *et al.* (1996).

2 THEORETICAL PRELIMINARIES

As a domain theoretical model of an asymmetric particle we consider geometrical configurations of prismatic particles with n domains as shown in Fig. 4 for $n=4$. These configurations are based on uniaxial anisotropy with the easy axis of magnetization lying in the same plane as the pair of parallel surfaces, which are part of the particle's boundary. The particles are further constrained to be magnetically hard. Thus they contain infinitely thin parallel planar domain walls. The wall normals are perpendicular to the normal of the back and front particle surfaces as well as to the easy axis. The equilibrium wall positions are obtained by minimizing the sum of wall energy, stray-field energy and external field energy,

$$E(\mathbf{x}) = \gamma_0 F(\mathbf{x}) + K_d V N(\mathbf{x}) - \mu_0 H M(\mathbf{x}) V . \quad (1)$$

Here γ_0 denotes the specific domain wall energy (J m^{-2}), $F(\mathbf{x})$ is the total wall area as a function of the vector of wall positions $\mathbf{x}=(x_1, \ldots, x_{n-1})$, $K_d = \mu_0 M_s^2/2$ is the characteristic stray-field energy coefficient, M_s is the saturation magnetization, V is the particle volume, $N(\mathbf{x})$ is the effective demagnetizing factor, H is the external field in the direction of the easy axis and $M(\mathbf{x})$ is the net magnetization.

The essential features of (1) are obtained by introducing reduced quantities, namely the characteristic material length $\lambda_0 := \gamma_0/K_d$, the reduced energy density $\varepsilon(\mathbf{x}) := E(\mathbf{x})/(K_d V)$, the reduced magnetization $m(\mathbf{x}) := M(\mathbf{x})/M_s$, the reduced particle size $L := V^{1/3}/\lambda_0$, the reduced wall area $\alpha(\mathbf{x}) := F(\mathbf{x})/V^{2/3}$, the reduced applied field $h := 2H/M_s$ and the reduced anisotropy constant $Q = K_u/K_d$, where K_u is the uniaxial magnetocrystalline anisotropy constant.

Inserting these quantities into (1) yields

$$\varepsilon(\mathbf{x}) = \alpha(\mathbf{x})/L + N(\mathbf{x}) - hm(\mathbf{x}) . \quad (2)$$

The only free parameter in this reduced representation is L. It represents the particle diameter in units of λ_0. All other quantities $[\alpha(\mathbf{x}), N(\mathbf{x}), m(\mathbf{x})]$ reflect only the particle shape and the relative positions of domain walls. The material parameters of the particle determine the scaling length λ_0, which is approximately 8 nm for unstressed magnetite and 80 nm for unstressed TM60 (approximate values of λ_0 for TM10 and TM30 are 12 and 20 nm, respectively). Assuming a high uniaxial internal stress of $\sigma_0 \approx 100$ MPa yields $\lambda_0 \approx 11$ nm for magnetite and 130 nm for TM60. Since the above model relies on the assumption that the wall width is small compared to particle size, it cannot be applied to small unstressed magnetite grains. Even though eq. (2) does not depend on Q, the model used to derive this equation implicitly assumes that $Q \gg 1$, since wall width and flux closure effects are neglected. Hence, for small Q our domain theoretical results have to be complemented by more rigorous 3-D calculations.

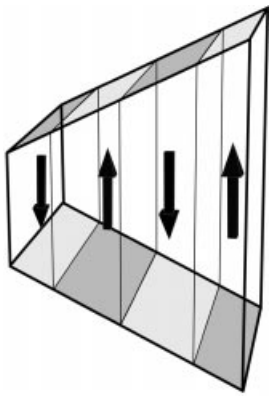

Figure 4. Sketch of an irregular prismatic uniaxial particle with $n=4$ domains. Front and back surfaces lie in parallel xy-planes, domain walls in parallel yz-planes. The easy axis corresponds to the y-direction. Magnetic surface charges occur only on the shaded surface regions.

3 ENERGY CALCULATION

3.1 Domain theoretical analysis

In the following the details of the energy computation for prismatic n-domain particles with an arbitrary convex base are elaborated. As usual, the most difficult part of the energy calculation is the calculation of the demagnetizing factor N as a function of the wall positions $x_1, \ldots, x_{n-1}$. For cuboid particles this is usually done by applying the Rhodes & Rowlands function (Rhodes & Rowlands 1954; Shcherbakov 1978; Dunlop 1983). Since we restrict ourselves to the more general but still specialized case of prismatic particles with uniaxial anisotropy parallel to the base of the prism, the problem amounts to finding the interaction coefficient between rectangular sides of a prismatic particle. The general form of such an interaction coefficient is

$$W_{S_1,S_2} = \int_{S_1}\int_{S_2} \frac{1}{|\mathbf{x}-\mathbf{y}|}\, d\mathbf{x}\, d\mathbf{y} .$$

Now a coordinate system is chosen such that with some $\mathbf{p}, \mathbf{v} \in \mathbb{R}^2$ we have

$$S_1 = [0, 1] \times \{0\} \times [0, h], \quad S_2 = \{\mathbf{p} + t\mathbf{v} : t \in [0, 1]\} \times [0, h] .$$

Fig. 5 sketches the geometric situation obtained. Using the notations of Fig. 5, the interaction coefficient can be

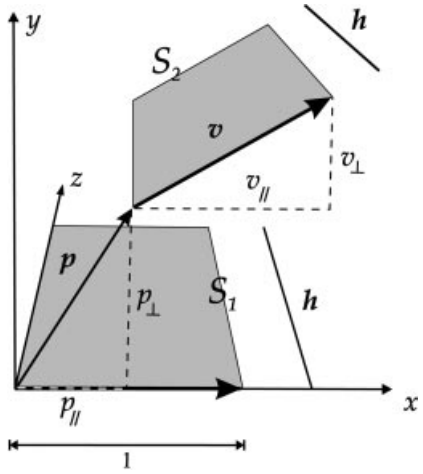

Figure 5. Geometric configuration for the calculation of interaction coefficients between magnetically charged rectangular sheets. Both sheets lie perpendicular to the xy-plane and have length h.

transformed to

$$W_{S_1,S_2} = \sqrt{v_\parallel^2+v_\perp^2}\int_{x=0}^{1}\int_{z=0}^{h}\int_{t=0}^{1}\int_{\zeta=0}^{h} \times \frac{1}{\sqrt{(x-p_\parallel-tv_\parallel)^2+(p_\perp+tv_\perp)^2+(z-\zeta)^2}}\,d\zeta\,dt\,dz\,dx$$
$$= h^2\sqrt{v_\parallel^2+v_\perp^2} \times \int_{t=0}^{1} F_{210}(h(z-\zeta),\, x-p_\parallel-tv_\parallel,\, p_\perp+tv_\perp)\big|_{z,\zeta,x=0}^{1}\,dt\,. \quad (3)$$

With the abbreviation $r=\sqrt{x^2+y^2+z^2}$, the function F_{210} is given by

$$F_{210}(x,y,z) = xy\log(x+r)+\frac{x^2-z^2}{2}\log(y+r) - x\arctan\left(\frac{xy}{zr}\right)-\frac{yr}{2}\,. \quad (4)$$

This formula is derived in an analogous way to that in Ramstöck *et al.* (1994) or Fabian *et al.* (1996). Shcherbakov *et al.* (1997) obtained a similar expression for quadratic surfaces. Each coefficient can now be calculated by a 1-D numerical integration of (3).

Using these coefficients, the calculation of the demagnetizing factor for a prism with walls parallel to the *yz*-plane at positions $x_1, \ldots, x_{n-1}$ is readily manageable. A model such as that in Fig. 4 consists of a set of M rectangular charged sheets $S_1, \ldots, S_M$, where the surface charge $\sigma_i = \mathbf{m}\cdot\mathbf{n_i}$ is defined to be the scalar product of the magnetization of the adjacent domain and the exterior surface normal of S_i. The effective demagnetizing factor is now given by

$$N(x_1, \ldots, x_{n-1}) = \sum_{i,j=1}^{M}\sigma_i\sigma_j W_{S_i,S_j}\,. \quad (5)$$

Note that the self-interaction coefficients W_{S_i,S_i} of the rectangles can even be calculated analytically. They form special cases of $W_\parallel$ as given in eqs (21)–(23) of Fabian *et al.* (1996).

4 RESULTS FOR HIGH-ANISOTROPY PARTICLES

In order to investigate the influence of particle shape upon equilibrium remanence, we first choose a family of prismatic particles $T(a,b,c,d) := B_T(b,c,d)\times\{0,a\}$, where

$$B_T(b,c,d) := \text{convex hull}[(0,0),(b,-d),(b,c),(0,c-d)]$$

is the trapezoidal base of the prism. Now $T(1,1,1,d)$ is a one-parameter family of particles having volume 1, the end-members of which are a cubic particle at $d=0$ and a triangular prism at $d=1$.

Fig. 6 collects equilibrium energy and remanence as a function of grain size L for a number of particles in this family. Equilibrium states have been calculated assuming uniaxial anisotropy with y as the easy direction for up to four domains.

Since cubic particles with an even number of domains carry zero equilibrium remanence, it is remarkable that even for the least asymmetric case $d=0.1$ in Fig. 6 one finds two-domain remanences above 0.05 and four-domain remanences of 0.016–0.017. For $d=0.3$ the two-domain remanence of ≈ 0.2 is already larger than the three-domain remanence, and for more irregular grains, two-domain remanences of more than 0.5 are not unusual.

It should be noted that due to the prismatic structure even the most asymmetric of the particles investigated here are still relatively regular when compared to general particle shapes with 3-D corners such as the octahedral particle in Fig. 7. However, the moderate deviation from the symmetric shape investigated here already generates strong effects. The particle remanences in the equilibrium state as a function of grain size are collected in the bilogarithmic plot in Fig. 8. The remanence decreases beyond the SD state approximately with $L^{-0.8}$ to L^{-1}. For the asymmetric particles with $d\geq 0.5$ this trend is easily recognizable, while in more symmetric particles the overall power law which governs remanence decrease is obscured by the pronounced downward steps at even domain numbers. The power law of the decrease proves to be nearly independent of the details of particle shape. Fig. 9 shows that for different triangular prisms the same power law is obtained. The variation in shape induces a shift of the bilogarithmic curves rather than a relative tilt.

Because of the computational effort involved, our calculations are limited to four domain states. This effectively restricts the investigated particle size for stressed magnetite (100 MPa) to less than 1 μm and to less than 5 μm for TM60. While there is no indication that the approximate power law might break down for larger grain sizes, this claim should be substantiated by further computations.

5 DISCUSSION

The results of our calculations show that domain imbalance is an inherent remanence mechanism for almost all particle geometries. Asymmetric grain shape generates a considerable remanence not only in particles with an odd number of domains, but in all kinds of domain structures.

The observed domain imbalance moments decrease with grain size on average as $L^{-\alpha}$, where α assumes values between 0.8 and 1.0. This grain-size dependence corresponds well to the experimental findings for PSD remanences (see Dunlop & Özdemir 1997).

5.1 Domain imbalance moments are single-domain-like

Of primary importance for the validity of the proposal that domain imbalance accounts for an SD-like part of PSD remanence is the question whether it is sufficiently stable and of high coercivity. Its stability becomes evident by noting that remanence due to domain imbalance—similar to SD remanence—is a *global* remanence, which means that it is carried by the overall structure and not by single local features. The inherent domain imbalance is global, because it reverses only if *all* domains of the particle reverse. Domain imbalance of the remanent state cannot be reversed by wall movements or other local structural changes, yet global remanence can still be overprinted or enhanced by local remanence mechanisms such as wall pinning or metastability, which then leads to mixed remanence phenomena as observed in TRM and LTD properties of PSD particles.

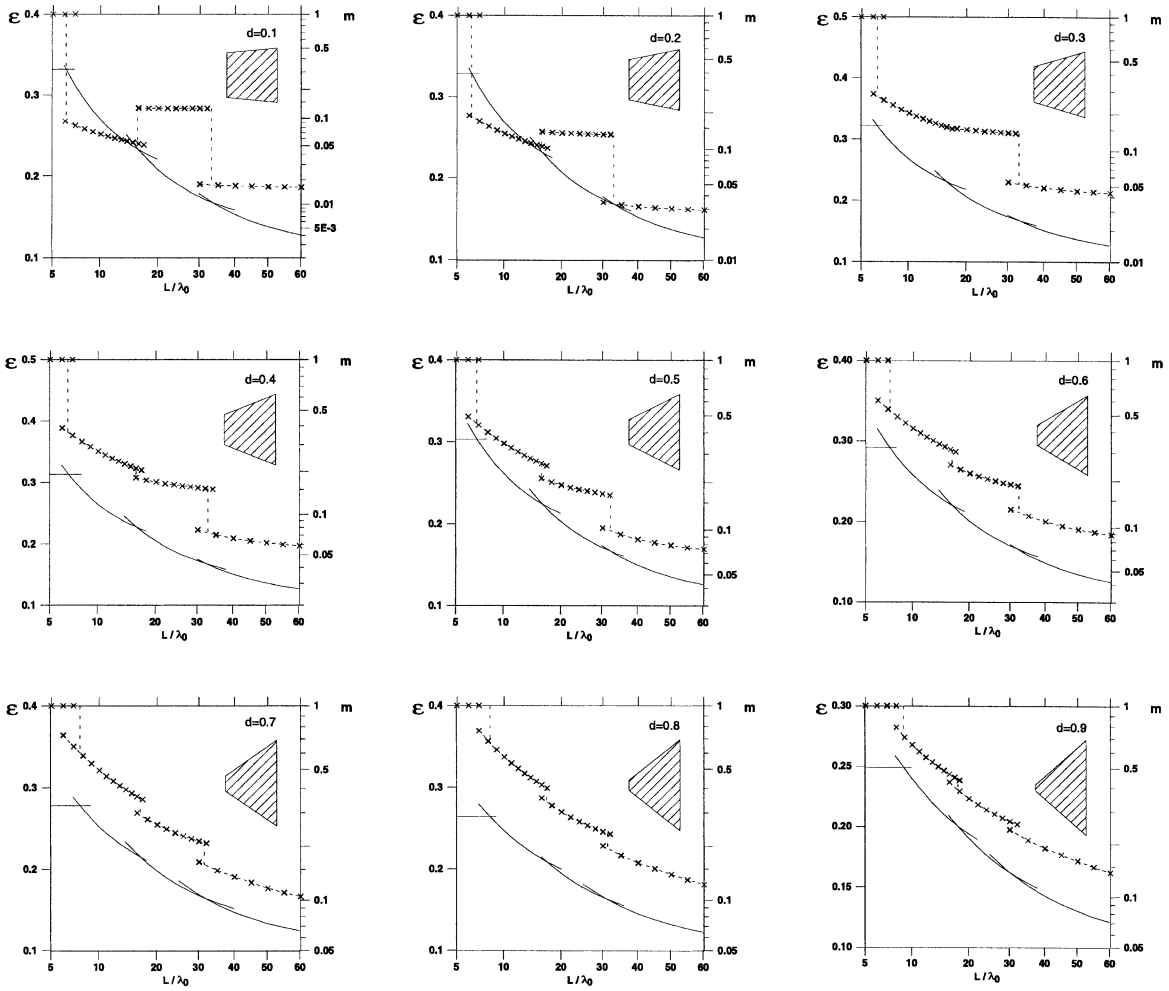

Figure 6. Energy ε in units of $[K_d V]$ (solid lines) and remanence m (dashed lines with crosses) of trapezoidal particles $T(1, 1, 1, d)$ with $d = 0.1, \ldots, 0.9$ as a function of L. The values for SD, two-, three- and four-domain equilibrium states are shown.

The characteristic coercivity feature of SD particles is the high median destructive field (MDF) $H_{1/2}$ of the AF demagnetization curve. A detailed prediction of the AF stability of shape-induced domain imbalance moments would

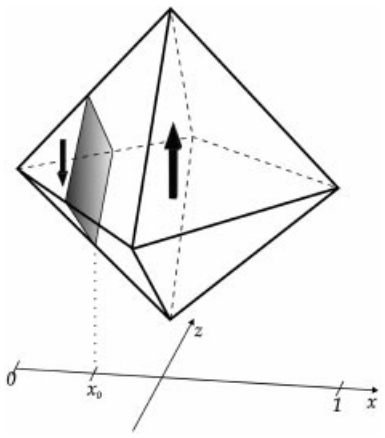

Figure 7. Example of a fully 3-D corner in an octahedral particle with uniaxial anisotropy. The wall energy in this case depends quadratically on x_0. Such corners do not occur for our prismatic particles, where the wall energy depends only linearly on the wall position.

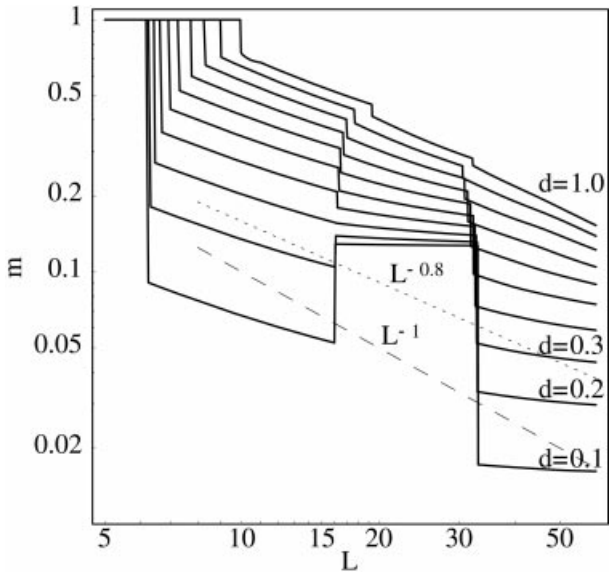

Figure 8. Bilogarithmic plot of equilibrium remanence m against grain size L in units of λ_0. Each curve corresponds to a trapezoidal particle $T(1, 1, 1, d)$, with $d = 0.1, 0.2, \ldots, 1.0$. For particles with $d \geq 0.3$, m decreases monotonously with L. The average rate of decrease appears to lie between $L^{-0.8}$ (dotted line) and L^{-1} (dashed line).

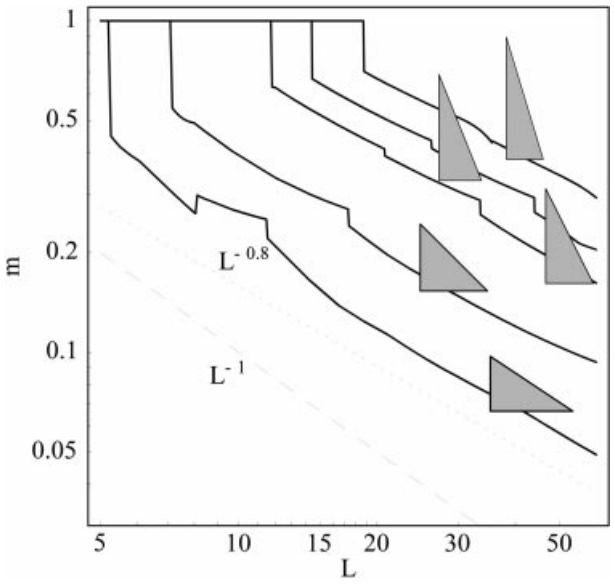

Figure 9. Bilogarithmic plot of equilibrium remanence m against grain size L in units of λ_0 for triangular prisms of volume 1 and height 1. Again the average rate of decrease lies between $L^{-0.8}$ (dotted line) and L^{-1} (dashed line).

require inclusion of the nucleation processes, which is not yet achievable. However, we can estimate the field which is needed to remove the domain imbalance moment of a two-domain particle. Its remanence can only be removed if the particle becomes saturated during the AF treatment, otherwise the equilibrium state after demagnetization cannot be inverted. Fig. 10 compares the energies of single-domain and two-domain states of a $T(1, 1, 1, 1/2)$ particle with $L=15$ as a function of an external field h pointing along the easy axis. Between the critical field values $h^-_{\rm crit} < h < h^+_{\rm crit}$, the two-domain structure is the absolute energy minimum. If the AF peak field is smaller than $\min(|h^-_{\rm crit}|, |h^+_{\rm crit}|)$ the particle is not saturated during the demagnetization and the shape-induced remanence cannot be removed. The remanence will certainly

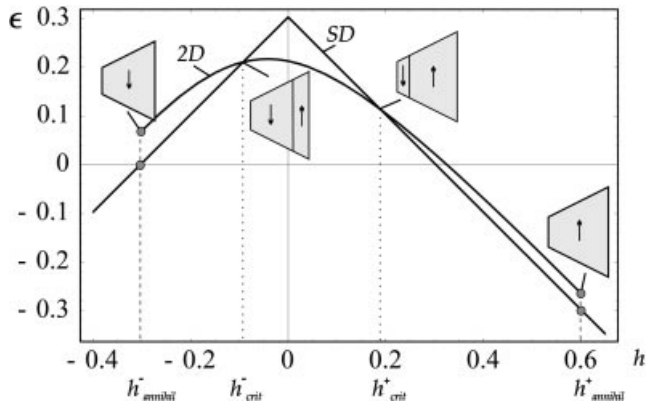

Figure 10. Energies of SD and two-domain states in a $T(1, 1, 1, 1/2)$ particle with $L=15$ as a function of an external field h. The field direction coincides with the easy axis. At the critical fields $h^{\pm}_{\rm crit}$ the absolute energy minimum changes from two-domain to SD. At $h^{\pm}_{\rm annihil}$ the metastable two-domain states become unstable. The numerical values are $h^-_{\rm crit} = -0.094, h^+_{\rm crit} = 0.189, h^-_{\rm annihil} = -0.304, h^+_{\rm annihil} = 0.6055$.

be removed as soon as the AF peak field exceeds either $h^-_{\rm annihil}$ or $h^+_{\rm annihil}$, where the equilibrium wall position coincides with the particle surface and the wall is annihilated. At the annihilation fields $h^{\pm}_{\rm annihil}$, the offset between the SD and two-domain energy curves in Fig. 10 corresponds to the additional wall energy.

A lower bound for the AF peak field necessary to remove the shape-induced remanence of the above particle is $|h^-_{\rm crit}| \approx 0.09$ (which for magnetite would give about 28 mT). This roughly corresponds to the switching field for coherent rotation of a prolate SD magnetite particle ($Q = K_1/K_{\rm d} \approx 0.01$, where K_1 is the first cubic magnetocrystalline anisotropy constant) with elongation $q=1.1$. Using $h^-_{\rm annihil}$ as an upper bound for the above AF peak field yields an AF demagnetization curve that corresponds to an SD particle with $q \approx 1.4$.

In Fig. 10 it can be seen that saturation of the two-domain particle occurs at lower field intensities when the field pushes the wall towards the long edge of the trapezoid. Because this movement increases the wall energy and because a larger volume has to be magnetically inverted, it seems at first glance paradoxical that it is performed at a smaller field intensity.

The stability of equilibrium remanence due to shape-induced domain imbalance with respect to thermal demagnetization depends on the variation of the material constants with temperature T. Since in the reduced form of the energy equation only the scaling length λ_0 depends on the material constants, the qualitative behaviour during thermal demagnetization corresponds to a shift of the reduced particle size $L(T)$ with temperature. For a particle with volume V the reduced particle diameter $L(T)$ is given by $L(T) = V^{1/3}/\lambda_0(T)$. For magnetite and titanomagnetite λ_0 increases with temperature. For our example particle $T(1, 1, 1, 1/2)$ with grain size $L(T_0)=15$ at room temperature T_0, the shape-induced remanence fraction according to Fig. 8 would therefore increase with temperature. For particles with more than two domains, the equilibrium remanence could reverse at points where the number of domains in the stable configuration decreases by one. However, whether walls actually nucleate or denucleate at transition sizes for equilibrium states is not predictable from our results.

Further evidence for the validity of our claim that shape-induced domain imbalance is a main contribution to the SD-like part of PSD remanence is its stress dependence, which follows from the above theory. In eq. (2) all lengths are measured in relation to the characteristic length λ_0. Since the wall energy γ_0 is in good approximation given by $\gamma_0 \approx 4\sqrt{AK}$ and since the predominant anisotropy K depends approximately linearly on stress σ, there is a dependence $\lambda_0 \sim \sqrt{\sigma}$ as soon as stress-induced anisotropy is large in comparison to magnetocrystalline anisotropy. Stress therefore only rescales the relevant lengths, without changing the overall effect of domain imbalance. This is in perfect agreement with the observation that stress affects the grain-size dependence of $M_{\rm rs}$ and $H_{\rm c}$ by shifting the unstressed values horizontally on a log–log diagram. This shift exactly corresponds to length rescaling. The slight change in the slope of the observed dependences might be due to the fact that highly stressed grains on average also have more irregular shapes than unstressed particles. Data for the latter have mainly been obtained using particles with highly symmetric shapes of grown crystals (e.g. Heider *et al.* 1987; Heider & Bryndzia 1987).

5.2 Low-temperature memory

Shape-induced domain imbalance may also be responsible for some of the experimentally observed properties of LT memory in magnetite. All evidence of LT memory seems to indicate that its origins are either large SD particles or stress-dominated regions which are not influenced by the zero of $K_1(T)$ at the isotropic temperature T_{iso}. While these mechanisms explain that remanence can survive LTD treatment, they cannot account for recovery of remanence which was lost below the isotropic point and occurs again when heating up to room temperature as reported by Kobayashi & Fuller (1968), Hodych (1991), Hodych *et al.* (1998), Heider *et al.* (1992) and Halgedahl & Jarrard (1995). The problem is that remanence due to strongly pinned walls or even domains which is overprinted below T_{iso} would also be shielded after reheating by newly formed soft walls.

Domain imbalance moments offer a way out of this problem for the theoretical explanation of LT memory (Fig. 11). Assume a PSD or MD particle where parts of the domain structure are stress-controlled whilst most of the grain is controlled by magnetocrystalline anisotropy. Close to the isotropic temperature nearly all local remanence (for example, due to wall pinning) is deleted as is revealed by the occurrence of large Barkhausen jumps (Halgedahl & Jarrard 1995). Global remanence, however, remains and changes only its magnitude due to the varying material constants. Below T_{iso}, large parts of the domain structure are reorganized because of the change in magnetocrystalline anisotropy. Only stress-controlled regions remain unchanged. On heating back to room temperature these stress-controlled regions ensure that the former domain imbalance remanence—and not its reversed state—is re-established. Since domain imbalance is an equilibrium remanence, the problem of magnetic shielding does not appear. Global remanence can be completely recovered by returning to the initial temperature. Therefore, the LT memory of PSD or MD particles in this scenario consists of the global (domain imbalance) remanence contribution to the total remanence. Since the global remanence fraction is more stable than local remanences, the above model matches the experimental findings of Dunlop & Argyle (1991), Heider *et al.* (1992), Argyle *et al.* (1994) and Shcherbakova *et al.* (1996). In particular, the observation of Shcherbakova *et al.* (1996) that the pTRM of PSD and MD particles after LT demagnetization does not behave in an SD-like manner agrees more with the above model than with the assumption of metastable SD particles or SD-like inclusions.

6 CONCLUSIONS

In view of our results it seems likely that shape-induced domain imbalance contributes substantially to the SD-like fraction of the overall PSD remanence. This contribution has previously been underestimated, since all theoretical models were developed for the mathematically simpler case of highly symmetrical particles. In such particles domain imbalance is largely reduced.

Global remanence due to shape-induced domain imbalance can be mixed in nearly arbitrary fashion with local remanence fractions which stem from wall pinning or Barkhausen discreteness, surface anisotropy and other mechanisms whose presence is well established in multidomain material. Very irregular but homogeneous grains show mainly remanence due to domain imbalance, whilst perfectly symmetric (or very large) particles with high dislocation density possess mainly remanence due to Barkhausen discreteness.

PSD remanence due to wall moments or vortices can be the main source of remanence only for magnetically soft

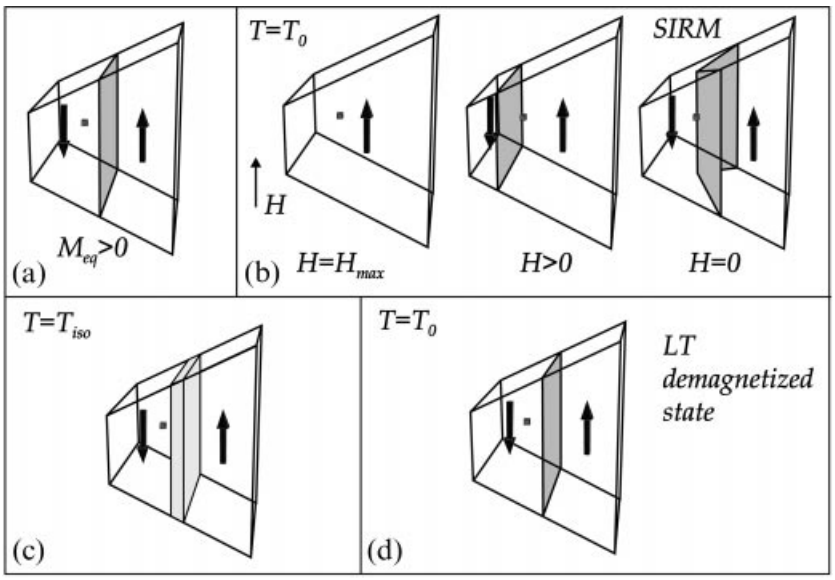

Figure 11. Model of a mechanism of LT memory. (a) The direction of the magnetostatic equilibrium magnetization M_{eq} is independent of the wall energy. (b) An acquired SIRM is the sum of the equilibrium magnetization and a superimposed magnetization which is due to pinning effects. (c) Cooling down to the isotropic temperature leads to an increase of domain widths and thereby unpins domain walls. The local contribution to the remanence is removed; the global equilibrium remanence remains. Below T_{iso} the domain structure is arbitrarily changed. However, if a part of the magnetization structure is fixed by stress the configuration shown—and not its inverse—is completely re-established when heating back to T_{iso}. (d) Heating to T_0 recovers M_{eq}, which is the global part of the original SIRM. The LT memory in this case corresponds to the magnetostatic equilibrium magnetization M_{eq}.

($Q \ll 1$) symmetric particles close to the SD–PSD transition. Preliminary 3-D micromagnetic calculations for asymmetric magnetite particles indicate that in asymmetric particles the remanence is also dominated by shape effects which interact in a complex manner with vortex moments. A detailed 3-D investigation of shape-induced PSD moments is in progress. Such calculations are of primary importance in investigating the influence of shape in equidimensional magnetite particles such as the hydrothermally grown crystals of Heider & Bryndzia (1987). The recent investigation of oblate octahedral particles by Williams & Wright (1998) indicates that 3-D micromagnetic models are capable of reproducing the respective experimental data.

The experimental evidence from LTD exhibits best the character of PSD remanence as a mixture of *global* (or SD-like) and *local* (or MD-like) remanences. This is in accordance with the proposed theory. Moreover, in terms of domain imbalance PSD moments it is possible to give a theoretical model for an LT memory process which shows recovery of remanence.

An interesting subsidiary aspect concerns the mechanism of remanence enhancement by stress. Shape-induced remanence increases due to a stress-induced increase in relative wall energy, which tends to move the walls into the corners of the particle. A further point of interest is that domain imbalance remanence can only be magnetically 'screened' by pinned walls, which induce local remanence opposite to the global imbalance moment. Easily movable walls cannot shield the domain imbalance moment because it is inherent to the equilibrium state of the particle.

Whilst the calculations presented prove that grain shape plays an important role in the equilibrium remanence of PSD particles, they only scratch the surface of the vast number of possible geometries. Since we restricted ourselves to prismatic particles, no truly 3-D particle corners (Fig. 7) have been considered. In 3-D corners the wall energy depends quadratically on the wall position. The shape effect on equilibrium remanence will therefore be even more pronounced than in the cases presented here. The measured grain-size dependences of M_{rs} and other quantities are averages over a wide variety of different particle shapes. Whilst our calculations seem to indicate that the exponent of the bilogarithmic size dependence is not strongly influenced by the details of the shape asymmetry, a thorough statistical analysis would be profitable.

ACKNOWLEDGMENTS

Major parts of this work were presented at the DGG meeting in Göttingen, 1998, and the 6th Castle meeting in Hruba Skala, 1998. An outline of this work is also included in Section 5.7.2 of Hubert & Schäfer (1998). The comments of V. P. Shcherbakov and an anonymous reviewer significantly improved the manuscript. We thank A. Newell, W. Williams and M. Winklhofer for fruitful discussions.

The second author, AH, passed away whilst the manuscript was under review. The first author alone is responsible for any remaining errors or misconceptions in the final version.

REFERENCES

Argyle, K.S., Dunlop, D.J. & Xu, S., 1994. Single-domain behaviour of multidomain magnetite grains (abstract), *EOS, Trans. Am. geophys. Un.,* **75,** Fall Mtng suppl., 196.

Banerjee, S.K., 1977. On the origin of stable remanence in pseudo-single domain grains, *J. Geomag. Geoelectr.,* **29,** 319–329.

Craik, D.J. & McIntyre, D.A., 1969. Anhysteretic magnetization processes in multidomain crystals and polycrystals, *Proc. R. Soc. Lond.,* **313,** 97–116.

Dunlop, D., 1973. Superparamagnetic and single-domain threshold sizes in magnetite, *J. geophys. Res.,* **78,** 1780–1793.

Dunlop, D., 1995. Magnetism in rocks, *J. geophys. Res.,* **100,** 2161–2174.

Dunlop, D. & Argyle, K., 1991. Separating multidomain and single-domain-like remanences in pseudo-single-domain magnetites (215–540 nm) by low-temperature demagnetization, *J. geophys. Res.,* **96,** 2007–2017.

Dunlop, D.J., 1977. The hunting of the 'PSARK', *J. Geomag. Geoelectr.,* **29,** 293–318.

Dunlop, D.J., 1983. On the demagnetizing energy and demagnetizing factor of a multidomain ferromagnetic cube, *Geophys. Res. Lett.,* **10,** 79–82.

Dunlop, D.J., 1990. Developments in rock magnetism, *Rep. Prog. Phys.,* **53,** 707–792.

Dunlop, D.J. & Özdemir, O., 1997. *Rock Magnetism,* Cambridge University Press, Cambridge.

Enkin, R.J. & Dunlop, D., 1987. A micromagnetic study of pseudo-single-domain remanence in magnetite, *J. geophys. Res.,* **92,** 12 726–12 740.

Fabian, K. & Heider, F., 1996. How to include magnetostriction in micromagnetic models of titanomagnetite grains, *Geophys. Res. Lett.,* **23,** 2839–2842.

Fabian, K., Kirchner, A., Williams, W., Heider, F., Leibl, T. & Hubert, A., 1996. Three-dimensional micromagnetic calculations for magnetite using FFT, *Geophys. J. Int.,* **124,** 89–104.

Geiß, C.E., Heider, F. & Soffel, H.C., 1996. Magnetic domain observation on magnetite and titanomaghemite grains (0.5–10 μm), *Geophys. J. Int.,* **124,** 75–88.

Halgedahl, S., 1991. Magnetic domain patterns observed on synthetic Ti-rich titanomagnetite as a function of temperature and in states of thermoremanent magnetization, *J. geophys. Res.,* **96,** 3943–3972.

Halgedahl, S. & Fuller, M., 1980. Magnetic domain observations of nucleation processes in fine particles of intermediate titanomagnetite, *Nature,* **288,** 70–72.

Halgedahl, S. & Fuller, M., 1983. The dependence of magnetic domain structure upon magnetization state with emphasis upon nucleation as a mechanism for pseudo-single-domain behavior, *J. geophys. Res.,* **88,** 6505–6522.

Halgedahl, S.L. & Jarrard, R.D., 1995. Low temperature behavior of single-domain through multidomain magnetite, *Earth planet. Sci. Lett.,* **130,** 127–139.

Heider, F. & Bryndzia, L.T., 1987. Hydrothermal growth of magnetite crystals (1 μm to 1 mm), *J. Cryst. Growth,* **84,** 50–56.

Heider, F., Dunlop, D.J. & Sugiura, N., 1987. Magnetic properties of hydrothermally recrystallized magnetite crystals, *Science,* **236,** 1287–1290.

Heider, F., Halgedahl, S.L. & Dunlop, D.J., 1988. Temperature dependence of magnetic domains in magnetite crystals, *Geophys. Res. Lett.,* **15,** 499–502.

Heider, F., Dunlop, D.J. & Soffel, H.C., 1992. Low-temperature and alternating field demagnetization of saturation remanence and thermoremanence in magnetite grains (0.037 μm to 5 mm), *J. geophys. Res.,* **97,** 9371–9381.

Hodych, J.P., 1991. Low-temperature demagnetization of saturation remanence in rocks bearing multidomain magnetite, *Phys. Earth planet. Inter.,* **66,** 144–152.

Hodych, J.P., Mackay, R.I. & English, G.M., 1998. Low-temperature demagnetization of saturation remanence in magnetite-bearing dolerites of high coercivity, *Geophys. J. Int.,* **132,** 401–411.

Hubert, A. & Schäfer, R., 1998. *Magnetic Domains,* Springer, Berlin.

Hunt, C.P., Moskowitz, B.M. & Banerjee, S.K., 1995. Magnetic properties of rocks and minerals, in *Rock Physics and Phase Relations,* pp. 189–204, AGU Reference shelf, Vol. 3, Washington.

Kobayashi, K. & Fuller, M., 1968. Stable remanence and memory of multi-domain materials with special reference to magnetite, *Phil. Mag.,* **18,** 601–624.

McClelland, E. & Shcherbakov, V., 1995. Metastability of domain state in multidomain magnetite: consequences for remanence acquisition, *J. geophys. Res.,* **100,** 3841–3857.

Moon, T. & Merrill, R., 1984. The magnetic moments of non-uniformly magnetized grains, *Phys. Earth planet. Inter.,* **34,** 186–194.

Ramstöck, K., Leibl, T. & Hubert, A., 1994. Optimizing stray field and exchange energy computations in finite-element micromagnetics, *J. Magn. Magn. Mater.,* **135,** 97–110.

Rhodes, P. & Rowlands, G., 1954. Demagnetising energies of uniformly magnetised rectangular blocks, *Proc. Leeds Phil. Lit. Soc.,* **6,** 191–210.

Shcherbakov, V., 1978. Theory concerning the magnetic properties of pseudo-single domain grains, *Izv. Earth Phys.,* **14,** 356–362 (English translation).

Shcherbakov, V.P., Winklhofer, M., Hanzlik, M. & Petersen, N., 1997. Elastic stability of chains of magnetosomes in magnetotactic bacteria, *Eur. Biophys. J.,* **26,** 319–326.

Shcherbakova, V.V., Shcherbakov, V.P., Schmidt, P.W. & Prevot, M., 1996. On the effect of low-temperature demagnetization on TRMs and pTRMs, *Geophys. J. Int.,* **127,** 379–386.

Stacey, F., 1962. A generalized theory of thermoremanence, covering the transition from single domain to multi-domain magnetic grains, *Phil. Mag.,* **7,** 1887–1900.

Stacey, F.D., 1963. The physical theory of rock magnetism, *Adv. Phys.,* **12,** 45–133.

Stacey, F.D. & Banerjee, S.K., 1974. *The Physical Principles of Rock Magnetism,* Elsevier, Amsterdam.

Sugiura, N., 1988. On the origin of PSD moment in magnetite, *Geophys. J.,* **92,** 479–485.

Verhoogen, J., 1959. The origin of thermoremanent magnetization, *J. geophys. Res.,* **64,** 2441–2449.

Williams, W. & Dunlop, D., 1990. Some effects of grain shape and varying external magnetic fields on the magnetic structure of small grains of magnetite, *Phys. Earth planet. Inter.,* **65,** 1–14.

Williams, W. & Dunlop, D.J., 1989. Three-dimensional micromagnetic modelling of ferromagnetic domain structure, *Nature,* **337,** 634–637.

Williams, W. & Wright, T.M., 1998. High-resolution micromagnetic models of fine grains of magnetite, *J. geophys. Res.,* **103,** 30 537–30 550.

Xu, S. & Dunlop, D.J., 1993. Theory of alternating field demagnetization of multidomain grains and implications for the origin of pseudo-single-domain remanence, *J. geophys. Res.,* **98**(B3), 4183–4190.